THE JOURNAL OF BIOLOGICAL CHEMISTRY
Vol. 277, No. 37, Issue of September 13, pp. 34451–34461, 2002

Printed in U.S.A.

The Neurotoxin 1-Methyl-4-phenyl-1,2,3,6-tetrahydropyridine Induces Apoptosis in Mouse Nigrostriatal Glia

RELEVANCE TO NIGRAL NEURONAL DEATH AND STRIATAL NEUROCHEMICAL CHANGES*

Received for publication, March 4, 2002, and in revised form, May 30, 2002
Published, JBC Papers in Press, June 25, 2002, DOI 10.1074/jbc.M202099200

Pier Andrea Serra‡, Luigi Sciola§, Maria Rosaria Delogu‡, Alessandra Spano§, Gianni Monaco§, Egidio Miele‡, Gaia Rocchitta‡, Maddalena Miele‡, Rossana Migheli‡, and Maria Speranza Desole‡¶

From the ‡Department of Pharmacology and §Department of Physiological, Biochemical and Cellular Sciences, University of Sassari, 07100 Sassari, Italy

Swiss mice were given 1-methyl-4-phenyl-1,2,3,6-tetrahydropyridine (MPTP), 25 mg/kg/day, for 5 consecutive days and killed at different days after MPTP discontinuance. Decreases in striatal tyrosine hydroxylase activity and levels of dopamine and its metabolites were observed 1 day after MPTP discontinuance. Ascorbic acid and glutamate levels had increased, dehydroascorbic acid and GSH decreased, whereas catabolites of high-energy phosphates (inosine, hypoxanthine, xanthine, and uric acid) were unchanged. In addition, gliosis was observed in both striatum and substantia nigra compacta (SNc). Sections of SNc showed some terminal deoxynucleotidyl transferase-mediated 2′-deoxyuridine 5′-triphosphate nick end labeling (TUNEL)-positive cells. Neurochemical parameters of dopaminergic activity showed a trend toward recovery 3 days after MPTP discontinuance. At this time point, TUNEL-positive cells were detected in SNc; some of them showed nuclei with neuronal morphology. A late (days 6–11) increase in striatal dopamine oxidative metabolism, ascorbic acid oxidative status, and catabolites of high-energy phosphates were observed concomitant with nigral neuron and nigrostriatal glial cell apoptotic death, as revealed by TUNEL, acridine orange, and Hoechst staining, and transmission electron microscopy. These data suggest that MPTP-induced activation/apoptotic death of glial cells plays a key role in the sequential linkage of neurochemical and cellular events leading to dopaminergic nigral neuron apoptotic death.

Parkinson's disease (PD)[1] is characterized by a selective loss of neurons in the substantia nigra compacta (SNc) and significant diminution of neostriatal content of dopamine and its major acidic metabolites dihydroxyphenylacetic acid (DOPAC) and homovanillic acid (HVA). Consequently, the functioning of the nigrostriatal dopaminergic system is impaired. Although cellular and molecular pathways leading to neuronal death in PD are still unknown, major biochemical processes such as oxidative stress and impaired energy metabolism are involved (for review, see Ref. 1). The neurotoxin 1-methyl-4-phenyl-1,2,3,6-tetrahydropyridine (MPTP) induces in man a clinical syndrome closely resembling PD and is widely employed as a Parkinson's disease model in experimental animals (2). Astrocytes are the primary site of bioactivation of the innocuous MPTP to the toxic metabolite 1-methyl-4-phenyl-pyridinium ion (MPP^+) via the monoamine oxidase-dependent formation of a dihydropyridinium intermediate (3). The dihydropyridinium intermediate is a reactive radical that undergoes autoxidation with formation of superoxide anion ($O_2^{\cdot-}$) and MPP^+. In addition, the dihydropyridinium intermediate readily crosses the cellular membrane and undergoes autoxidation also in the extracellular space to form additional $O_2^{\cdot-}$ and MPP^+ (3). MPTP-induced hydroxyl radical formation in the striatum and substantia nigra of the mouse has been shown *in vivo* (4); in addition, MPP^+ alone promotes reactive oxygen species (ROS) formation (5–7).

MPTP/MPP^+-induced neuronal death has been widely demonstrated in experimental animals, including rodents (8, 9). The mode of neuronal death has been extensively studied *in vitro*. MPTP and MPP^+ induce apoptosis in neuroblastoma cells (10), dopaminergic cell cultures (11, 12), and in PC12 cells (13). Only a few reports, however, have addressed the mode of MPTP-induced neuronal death *in vivo*. It has been demonstrated in mice (9) that MPTP can induce necrotic or apoptotic neuronal death according to the dosage schedule. Recent histological studies performed on brains from Parkinsonian patients suggest that nigral cell death could be apoptotic (14, 15). However, apoptotic degeneration of nigral dopaminergic neurons in PD disease is still a controversial issue (for review, see Ref. 16).

MPTP, besides damaging nigrostriatal neurons, induces glial activation (17). Glia plays a key role in the antioxidant defense of the brain (18); in addition, dopaminergic neurons in SNc, which degenerate in PD, can be maintained by the glial cell line-derived neurotrophic factor (19). Glial cell line-derived

* This work was supported by the University of Sassari (ex 60% fund). The costs of publication of this article were defrayed in part by the payment of page charges. This article must therefore be hereby marked "*advertisement*" in accordance with 18 U.S.C. Section 1734 solely to indicate this fact.

¶ To whom correspondence should be addressed: Dept. of Pharmacology, Faculty of Medicine, University of Sassari, Viale S. Pietro 43B, 07100 Sassari, Italy. Fax: 39-79-228-525; E-mail: Pharmaco@ssmain.uniss.it.

[1] The abbreviations used are: PD, Parkinson's disease; SNc, substantia nigra compacta; DOPAC, dihydroxyphenylacetic acid; HVA, homovanillic acid; MPTP, 1-methyl-4-phenyl-1,2,3,6-tetrahydropyridine; MPP^+, 1-methyl-4-phenylpyridinium ion; ROS, reactive oxygen species; GDNF, glial cell line-derived neurotrophic factor; L-DOPA, L-dihydroxyphenylalanine; TEM, transmission electron microscopy; TUNEL, terminal deoxynucleotidyl transferase-mediated 2′-deoxyuridine 5′-triphosphate nick end labeling; AO, acridine orange; GFAP, glial fibrillary acidic protein; 3-MT, 3-methoxytyramine; DHAA, dehydroascorbic acid; TH, tyrosine hydroxylase; HPLC, high performance liquid chromatography; NO, nitric oxide, PBS, phosphate-buffered saline; ANOVA, analysis of variance; DOPAC, dihydroxyphenylacetic acid.

neurotrophic factor induces both protective and restorative effects on the nigrostriatal dopaminergic system of MPTP-treated mice (20) and monkeys (21). All these findings suggest that glia plays an important role in protecting the functioning of the nigrostriatal dopaminergic system from MPTP toxicity. In reality, there is evidence suggesting that alterations in glial functioning may be an important contributor to the pathologic process that occurs in PD (22, 23). The purpose of this study was to determine: (i) whether MPTP might produce cell damage in nigrostriatal glial cells of the mouse besides that in dopaminergic neurons; (ii) whether the eventual cellular damage might be characteristic of changes leading to apoptosis; (iii) whether neuronal and glial damage might be correlated with MPTP-induced striatal neurochemical changes.

EXPERIMENTAL PROCEDURES

Animals—Experiments were conducted on 3-month-old Swiss mice (Morini strain, Reggio Emilia, Italy), body weight 20–25 g, maintained, under standard animal care conditions, on a 12-h day/night cycle and given food and water *ad libitum*. All studies were carried out in accordance with the European EC Directive 86/609 included in the Decreto number 116/1992 of the Italian Ministry of the Public Health.

Materials—MPTP (HCl) was purchased by Research Biochemical International, Natick, MA; L-dihydroxyphenilalanine (L-DOPA), tyrosine, dihydropteridine reductase, 2-amino-4-hydroxy-6,7-dimethyltetrahydropteridine, and nicotinamide dinucleotide phosphate, reduced form, were purchased by Sigma.

Drug Administration—Groups of 8 mice per time period received an intraperitoneal injection of MPTP-HCl, 30 mg/kg/day, at 24-h intervals on 5 consecutive days. This dosage is below that producing necrotic cell death (9). The control group ($n = 11$) was given a vehicle (saline, 2 ml/kg intraperitoneal). Mice were killed by decapitation at 1, 3, 6, 11, and 14 days after the last MPTP injection. Controls were killed after the last MPTP group. Heads were cooled by rapid immersion in liquid nitrogen. Thereafter, striata and SNc of both sides were rapidly removed as previously described (24). Whereas striata of the left side were frozen at −80 °C for subsequent HPLC determination of neurochemicals (24), striata and SNc of the right side were fixed with a freshly prepared paraformaldehyde solution (4% in PBS, pH 7.4) for light microscopy. Left SNc were fixed with 2.5% glutaraldehyde in 0.1 M cacodilate buffer for transmission electron microscopy (TEM).

Light Microscopy—After extensive washing, the fixed tissue fragments were dehydrated through a graded series of ethanol, then passed in xylene and embedded in paraffin. Specimens (5–7 μm) were washed in xylene and rehydrated according to standard protocols. Sections were either stained with hematoxylin/eosin, or used for terminal deoxynucleotidyl transferase-mediated 2′-deoxyuridine 5′-triphosphate nick end labeling (TUNEL); some sections were processed for fluorescence microscopy and therefore fluorochromized with acridine orange (AO) or Hoechst 33342.

TUNEL—Striatal and nigral sections were incubated, after rehydration, with proteinase K (20 μg/ml in Tris-HCl buffer, pH 7.4–8) for 15 min at 21 °C. The blocking of endogenous peroxidase was performed with a solution of 0.3% H_2O_2 in methanol. Sections were permeabilized by incubation with a solution of Triton X-100 0.1% in PBS and incubated with fluorescein-2′-deoxyuridine 5′-triphosphate and terminal deoxynucleotidyl transferase. Thereafter, sections were stained by an antifluorescein antibody conjugated with horseradish peroxidase and subsequently incubated with diaminobenzidine substrate to produce a dark brown precipitate. Stained sections were analyzed under light microscopy.

Glial Fibrillary Acidic Protein (GFAP) and TUNEL Double Staining—Astrocytes within the SNc were identified by means of GFAP immunocytochemistry. GFAP is the major component of intermediate filaments of astrocytes and is a common marker for astrocytes. Rehydrated sections were preincubated for 30 min with 0.1 M PBS containing 20% horse serum and 0.01 M Tween 20. Sections were incubated with: (i) a monoclonal anti-GFAP antibody (1:400, DAKO) overnight at room temperature; (ii) biotinylated anti-mouse IgG antibody (DAKO) for 30 min at room temperature; (iii) buffer containing 3% H_2O_2 to inactivate the endogenous peroxidases; (iv) alkaline phosphatase-labeled avidin (1:100) for 30 min at room temperature. Between incubation steps, sections were washed 3 times in 0.1 M PBS containing 0.001 M Tween 20. Phosphatase was visualized by fast red. At this point, sections were incubated with fluorescein-2′-deoxyuridine 5′-triphosphate and terminal deoxynucleotidyl transferase to characterize the apoptotic nucleus. Thereafter, sections were stained by an anti-fluorescein antibody conjugated with horseradish peroxidase and subsequently incubated with diaminobenzidine substrate to produce a dark brown precipitate. A series of stained sections were analyzed under light microscopy.

AO and Hoechst 33342 Staining—Striatal and nigral sections were defatted (9) in Tris-buffered phenol for 25 min followed by 10 min in chloroform/methanol (1:1). Sections were rinsed in 100% ethanol for 2 min, air dried, and then rinsed in freshly made 1% glacial acetic acid for 1 min followed by distilled water for 1 min. Sections were kept for 30 s in a 0.01% solution of AO in PBS (pH 6.2), rinsed in PBS with mild agitation, and then mounted in 95% glycerol in PBS for immediate viewing under excitation at 488 nm on a Nikon Optiphot microscope. Double-stranded DNA complexes with AO to emit maximally at 530 nm as a bright green fluorescence, whereas single-stranded RNA emits maximally at 640 nm as a bright orange-red fluorescence. Rehydrated sections were rinsed in PBS and then fluorochromized with Hoechst 33342 (5 μg/ml in PBS) for 45 min at room temperature. The specimens were observed with an epifluorescence microscope (Nikon Optiphot).

Hematoxylin/Eosin Staining—Gliosis was assessed by means of hematoxylin/eosin staining of rehydrated sections of striatum and SNc, using routine protocol. The presence of some morphological features, such as enlarged and vesicular nuclei with prominent nucleoli, and the presence of lengthened eosinophilic structures (Rosenthal fibers) were considered as a histopathological index of gliosis (25). The amount of both enlarged nuclei and Rosenthal fibers/microscopic field allowed us to quantify gliosis.

TEM—Fragments from SNc were fixed in 2.5% glutaraldehyde in 0.1 M cacodylate buffer (pH 7.4) for 3 h at 4 °C and washed with the same buffer containing 7% sucrose; the specimens were then post-fixed in 1% OsO_4 for 2 h at 4 °C and washed repeatedly in buffer. Thereafter, specimens were dehydrated in acetone, passed through propylene oxide, and finally embedded in epoxy resin (agar 100). Ultrathin section (60 nm) were collected on copper grids and stained with uranyl acetate and lead citrate. The specimens were observed with a Zeiss EM 109 at 50 kV.

HPLC Determination of Striatal Neurochemicals—Dopamine, DOPAC, HVA, 3-methoxytyramine (3-MT), ascorbic acid, dehydroascorbic acid (DHAA), glutamate, inosine, hypoxanthine, xanthine, and uric acid determinations were performed by HPLC according to methods previously described (24, 26). GSH was determined according to the enzymatic recycling method of Anderson (27). Striata of the left side were weighed and homogenized in 1% *meta*-H_3PO_4 containing 1 mM EDTA. After centrifugation (17,500 × *g* for 10 min at 4 °C), the supernatant was divided into five aliquots. The first was filtered and immediately injected into the HPLC system for dopamine, DOPAC, HVA, 3-MT, ascorbic acid, and uric acid determinations. HPLC with electrochemical detection was done with a high-pressure pump Varian 9001 with a Rheodyne injector, 15 cm × 4.6 mm inner diameter TSK-ODS-80 TM column, electrochemical detector BAS LC-4B, and integrator Spectra Physics SP 4290. The mobile phase 0.1 M was citric acid, 0.1 M K_2HPO_4, 1 mM EDTA, 5% MeOH, and 70 mg/liter sodium octylsulfate (pH 3.0), the flow rate was 1.2 ml/min and 10 μl of sample were injected. The second aliquot was adjusted to pH 7.0 with 45% K_2HPO_4 and 1% DL-homocysteine was added to reduce DHAA to ascorbic acid. The sample was incubated for 30 min at 25 °C, then adjusted to pH 3.0 with 30% *meta*-H_3PO_4, filtered, and injected (20 μl) for total ascorbic acid determination. DHAA concentration was calculated from the difference in ascorbic acid content between the first and second aliquot. The third aliquot was processed for GSH determination (26). Glutamate determinations were performed, on 20 μl of the fourth aliquot, by HPLC with fluorimetric detection with a Varian model 9010 gradient system (at 360 and 450 nm excitation and emission wavelengths) following derivatization with *o*-phthalaldehyde. Briefly, derivatized amino acids were separated on a Ultrasphere C18 high speed 75 × 4.6-mm Beckman column. A gradient was run from 26 mM Na_2HPO_4/acetonitrile (95:5) (pH 6.6 with H_3PO_4) to Na_2HPO_4/acetonitrile (70:30) in 20 min at a flow rate of 1.2 ml/min. On the fifth aliquot, inosine, hypoxanthine, and xanthine determinations were performed (26) directly by injecting 50 μl of the filtered supernatant using the above high-pressure pump, column ODS-80 TM and a similar precolumn, UV detector (254 nm), and integrator. The mobile phase was composed of two eluants: K_2HPO_4/MeOH (97:3).

Tyrosine Hydroxylase (TH) Activity—TH activity was assessed by measuring tyrosine conversion to L-DOPA, according to Pothos *et al.* (28). Groups of 3 mice per time period were given MPTP according to the above treatment schedule. Controls were given saline intraperitoneally. Mice were killed by decapitation at 1, 3, and 6 days after the last MPTP injection. Heads were cooled by rapid immersion in liquid nitro-

gen. Thereafter, striata of both sides of each animal were rapidly removed, pooled, weighed, and homogenized in 10 volumes of (w/v) ice-cold 0.05 M Tris-HCl buffer (pH 6.0), containing 0.2% Triton X-100 (v/v). Protein content was determined on a 50-μl aliquot of the homogenate according to Lowry *et al.* (29), whereas the remainder was centrifuged at 10,000 $\times$ *g* for 10 min. TH activity in the supernatant was determined at the incubation conditions as describe by Coyle (30). Fifty μl of the supernatant were added to 16-ml tubes containing the following reaction mixture: 10 μl of 1 M KH_2PO_4 buffer (pH 5.5), 1.100 units of catalase in 10 μl of distilled water, 5 μl of 6.4 mM 2-amino-4-hydroxy-6,7-dimethyltetrahydropteridine (freshly prepared in 0.005 M HCl), 10 μl of dihydropteridine reductase, 5 μl of 0.01 M nicotinamide dinucleotide phosphate, reduced form, 10 μl of 0.1 M mercaptoethanol, and 10 μl of 3 mM $FeSO_4$. The reaction was initiated by the addition of 10 μl of 2.0 mM tyrosine; the reaction mixtures was incubated for 10, 30, or 60 min at 37 °C. Experiments were done in triplicate. TH activity was assessed by HPLC-EC determination (as described above) of L-DOPA formed. The percentage variation was calculated on the basis of the total amount of L-DOPA formed at the 3 incubation time points indicated above.

Statistical Analysis—All values were expressed in nanomole or picomole of milligrams/protein and given as mean ± S.E. Biochemical data were analyzed using ANOVA with Student-Newman-Keuls's *t* test post-hoc analysis. In some instances (TH activity) unpaired *t* test was also used.

RESULTS

One Day after MPTP Discontinuance—Striatal dopamine and DOPAC + HVA levels had significantly decreased by about 58 and 60%, respectively, as compared with controls (Fig. 1, *panel A*); the (DOPAC + HVA)/dopamine ratio, which is a reliable index of dopamine turnover, did not statistically differ from controls (Fig. 1, *panel C*). 3-MT levels, which can be assumed to be an index of dopamine release (31), had significantly decreased by about 38% (Fig. 1, *panel B*). All these changes denote an impairment of the functioning of the dopaminergic system and may be related to the MPTP-induced decrease of TH activity (32). In fact, striatal TH activity, assessed by measuring tyrosine conversion to L-DOPA, had reduced by about 80%, as compared with controls (Fig. 2). Ascorbic acid (+15%) and glutamate (+33%) levels had significantly increased, whereas GSH (−28%) and DHAA (−33%) levels decreased. The DHAA/ascorbic acid ratio, which can be assumed to be a reliable index of the ascorbic acid oxidative status and ROS formation (33), had decreased by about 38% (Fig. 3, *panels A–D*). Inosine, hypoxanthine, xanthine, and uric acid levels, as well as the inosine/hypoxanthine ratio, were in the range of control values (Fig. 4, *panels A–D*). It is widely accepted that increases in regional brain inosine, hypoxanthine, xanthine, and uric acid levels reflect degradation of intracellular high-energy phosphates (26, 34). Therefore, the lack of changes in compounds associated with high-energy phosphate degradation denotes that at this time point MPTP did not yet induce energy failure.

At this time point (day 1), a moderate reactive gliosis, as revealed by the presence of some enlarged and vesicular nuclei with prominent nucleoli, as well as of eosinophilic Rosenthal fibers, was observed in both striatum and SNc (Fig. 5, *panels c* and *d*). The analysis of DNA fragmentation in striatal sections showed no signs of TUNEL positivity (Fig. 6, *panel a*), whereas some TUNEL-positive cells were detected in sections of SNc (Fig. 6, *panel b*). AO and Hoechst 33342 staining of SNc sections showed few pyknotic nuclei.

Three Days after MPTP Discontinuance—Striatal dopamine levels (Fig. 1, *panel A*) and TH activity (Fig. 2) showed a significant trend to recovery ($p < 0.05$, compared with day 1 values); DOPAC + HVA levels (Fig. 1, *panel A*) and the (DOPAC + HVA)/dopamine ratio (Fig. 1, *panel C*) were within the range of control values, whereas 3-MT levels were still significantly lower by about 35%, compared with controls (Fig. 1, *panel B*). Ascorbic acid and DHAA levels, as well as the DHAA/AA ratio, were within the range of control values (Fig. 3, *panels A*, *B*, and *D*). GSH (Fig. 3, *panel A*) and glutamate (Fig. 3, *panel C*) levels had significantly decreased by about 24% and increased by about 35%, respectively. Inosine, hypoxanthine, xanthine, and uric acid levels, as well as the inosine/hypoxanthine ratio, were still in the range of control values (Fig. 4, *panels A–D*).

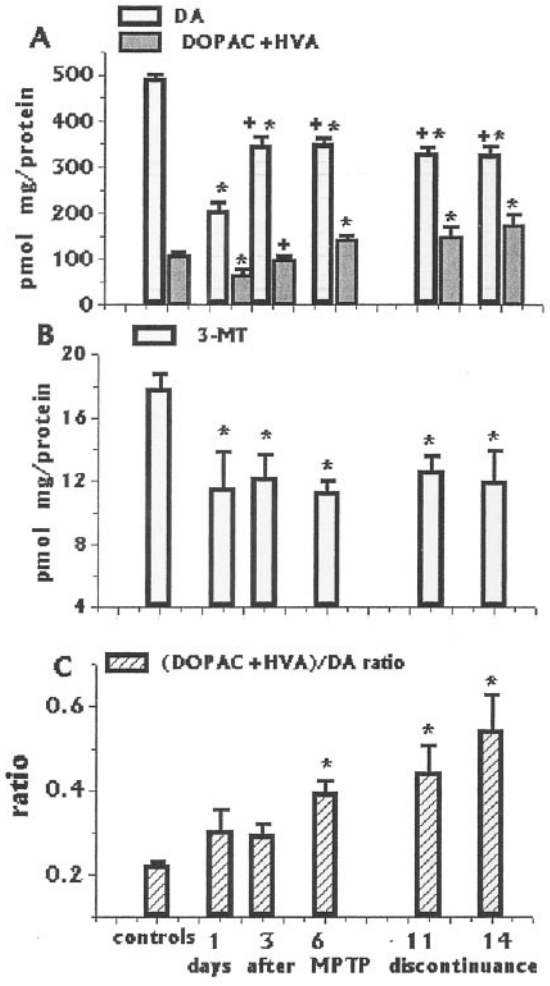

FIG. 1. **Levels of dopamine and DOPAC + HVA (*panel A*), 3-MT (*panel B*), and (DOPAC + HVA)/dopamine ratio (*panel C*) in the striatum of mice at different days after MPTP discontinuance.** Groups of 8 mice per time period received intraperitoneal injections of MPTP-HCl, 30 mg/kg/day, at 24-h intervals on 5 consecutive days. Mice were killed on the indicated days after MPTP discontinuance. Striatal neurochemicals determinations were performed by HPLC on striata of the *left side*. The control group ($n = 11$) was given saline. Values are given as mean ± S.E. *, $p < 0.05$ *versus* controls, and +, $p < .05$ *versus* day 1 (ANOVA followed by Student-Neuman-Keul's post-hoc comparison).

At this time point (day 3), striatal gliosis was more intense than on day 1 in both striatum and SNc, as revealed by the presence of several enlarged and vesicular cell nuclei with prominent nucleoli and eosinophilic Rosenthal fibers thicker than those seen on day 1. No signs of TUNEL positivity were detected in striatum sections (Fig. 6, *panel c*). In SNc sections several TUNEL- and GFAP-positive cells were observed. In addition, some nuclei with neuronal morphology showing light TUNEL positivity were detected (Fig. 6, *panel d*). Hoechst 33342 staining of SNc sections showed glial cells with pyknotic nuclei or condensed chromatin (apoptotic features), and neurons with presumptive normal morphology (Fig. 7, *panel c*). AO staining of SNc sections showed several glial cells with con-

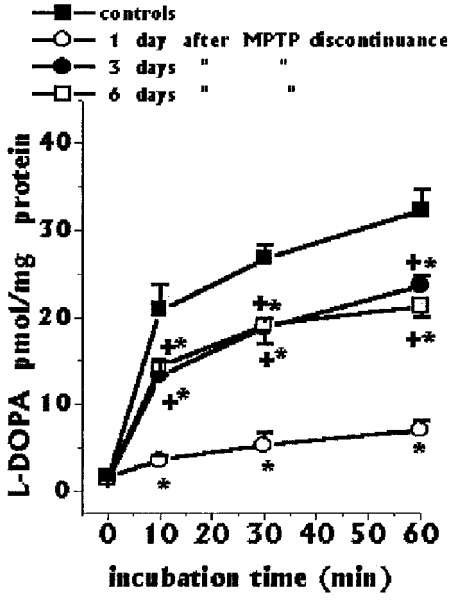

FIG. 2. **TH activity in the striatum of mice at different days after MPTP discontinuance.** Groups of 3 mice per time period were given intraperitoneal injections of MPTP-HCl, 30 mg/kg/day, at 24-h intervals on 5 consecutive days. The controls were given saline. Mice were killed by decapitation at 1, 3, and 6 days after the last MPTP injection. TH activity was assessed by measuring tyrosine conversion to L-DOPA in pooled striata of both sides of each animal. The reaction was initiated by the addition of 10 μl of 2.0 mM tyrosine, and the reaction mixture was incubated for 10, 30, or 60 min at 37 °C. Experiments were done in triplicate. Values are given as mean ± S.E. *, $p < 0.05$ *versus* controls, and +, $p < 0.05$ *versus* day 1 (ANOVA followed by Student-Neuman-Keul's post-hoc comparison and unpaired *t* test).

densed chromatin (apopoptic feature), and some neuronal cells with bright orange cytoplasmic fluorescence (presumptive of cellular integrity) (Fig. 7, *panel d*).

Six Days after MPTP Discontinuance—Striatal dopamine levels (Fig. 1, *panel A*) and TH activity (Fig. 2) did not recover further. DOPAC + HVA levels (Fig. 1, *panel A*) and the (DOPAC + HVA)/dopamine ratio (Fig. 1, *panel C*) significantly increased by about 25 and 76%, respectively, compared with controls. 3-MT levels were still significantly lower by about 44% (Fig. 1, *panel B*). Ascorbic levels were within the control range, whereas the DHAA and DHAA/ascorbic acid ratio increased by 26 and 33%, respectively (Fig. 3, *panels A*, *B*, and *D*). GSH (Fig. 3, *panel A*) and glutamate (Fig. 3, *panel C*) levels still showed a decrease of about 24% and an increase of about 44%, respectively. In addition, all compounds associated with high-energy phosphate degradation were significantly increased: inosine by 55%, hypoxanthine by 110%, xanthine by 195%, and uric acid by 71% (Fig. 4, *panels A*, *C*, and *D*). The increase in all compounds associated with high-energy phosphate degradation denotes that at this time point MPTP did indeed induce energy failure. The inosine/hypoxanthine ratio was significantly decreased, as a consequence of an increase in hypoxanthine levels greater than inosine (Fig. 4, *panel B*). Under physiological conditions, hypoxanthine is converted to inosinic acid by the salvage purine enzyme hypoxanthine-guanine phosphoribosyltransferase (EC 2.4.2.8); the proportion of hypoxanthine converted to inosinic acid is greater than that degraded to xanthine and uric acid by xanthine oxidase (EC 1.1.3.22) (35); in addition, hypoxanthine and inosine are incorporated into nucleotides at a similar rate (36). In some conditions, for instance in the aging brain (37), reutilization of preformed hypoxanthine prevails on *de novo* production of new purines to allow the cells to maintain their nucleotide pool. The increase in hypoxanthine greater than inosine levels denotes that MPTP might impair the incorporation in nucleotides of inosinic acid formed by the salvage purine enzyme hypoxanthine-guanine phosphoribosyltransferase; consequently, inosinic acid might be degraded again to inosine and then to hypoxanthine (26, 37). In addition, all of the above striatal neurochemical changes denote a condition of increases in ROS formation, as revealed by increases in the DHAA/ascorbic acid ratio (33), dopamine oxidative metabolism (38–40), as well as hypoxanthine and xanthine oxidative metabolism (41, 42).

At this time point (day 6), gliosis was more intense than on day 3 in both striatum and SNc. Sections of both regions, besides several enlarged and vesicular cell nuclei with prominent nucleoli, showed extensive areas of eosinophilic structures (Rosenthal fibers), indicative of astrocytes arranged in fascicles (Fig. 5, *panels e* and *f*). In contrast to day 3, striatal sections showed several TUNEL-positive cells (Fig. 6, *panel e*). Thus, the detection of TUNEL-positive cells in the striatum was concomitant with increases in all compounds associated with high-energy phosphate degradation. Furthermore, the number of TUNEL-positive cell nuclei of heterogeneous size in SNc greatly increased as compared with day 3 (Fig. 6, *panel f*). Hoechst 33342 staining of SNc sections showed glial cells with apparent clumps of hypercondensed chromatin and neurons with nuclear fragmentation (apoptotic features) (Fig. 7, *panel e*). AO staining of SNc sections showed several glial cells with condensed chromatin (apopoptic feature), and neurons with condensed chromatin margination at the nuclear periphery associated with pericellular space formation created by cell shrinkage (apoptotic features); in addition, the lack of orange cytoplasmic fluorescence is presumptive of cellular impairment (Fig. 7, *panel f*). TEM revealed nuclear chromatin condensation with apoptotic features in pigmented neurons (Fig. 8) and glial cells (Fig. 9). GFAP/TUNEL double staining revealed the astrocytic involvement in the apoptotic process (Fig. 10).

Eleven Days after MPTP Discontinuance—Striatal dopamine and 3-MT levels (Fig. 1, *panels A* and *B*) were still significantly lower than controls by about 33 and 27%, respectively. DOPAC + HVA levels and the (DOPAC + HVA)/dopamine ratio (Fig. 1, *panels A* and *C*) increased by about 36 and 97%, respectively. GSH levels still showed a significant decrease of about 26% (Fig. 3, *panel A*), whereas glutamate content had significantly increased by about 48% (Fig. 3, *panel C*). Ascorbic acid levels had decreased by about 13% (Fig. 3, *panel A*), whereas DHAA levels increased by about 46% (Fig. 3, *panel B*); consequently, the DHAA/AA ratio increased by about 78% (Fig. 3, *panel D*). Inosine, hypoxanthine, xanthine, and uric acid levels further increased to up to 74, 157, 243, and 163%, respectively, compared with controls (Fig. 4, *panels A*, *C*, and *D*). The inosine/hypoxanthine ratio was significantly decreased (Fig. 4, *panel B*).

At this time point (day 11), both striatal and nigral gliosis showed a trend toward subsidence, compared with day 6, as revealed by the apparent reduction of extensive areas of eosinophilic structures. The number of TUNEL-positive cells in the striatum (Fig. 6, *panel g*) was somewhat greater than on day 6. Again, the increase in the number of TUNEL-positive cells in the striatum was concomitant with a further increase in all compounds associated with high-energy phosphate degradation. The number of TUNEL-positive cells in the SNc was in the range of that on day 6. Some TUNEL-positive cells showed nuclei with neuronal morphology (Fig. 6, *panel h*). AO and Hoechst 33342 staining of SNc sections showed glial and neuronal cells with features similar to those shown in Fig. 7, *panels e* and f (day 6).

Fourteen Days after MPTP Discontinuance—At this time point, the decrease in striatal dopamine and 3-MT levels appeared to be stable (by about 33 and 27%, respectively, com-

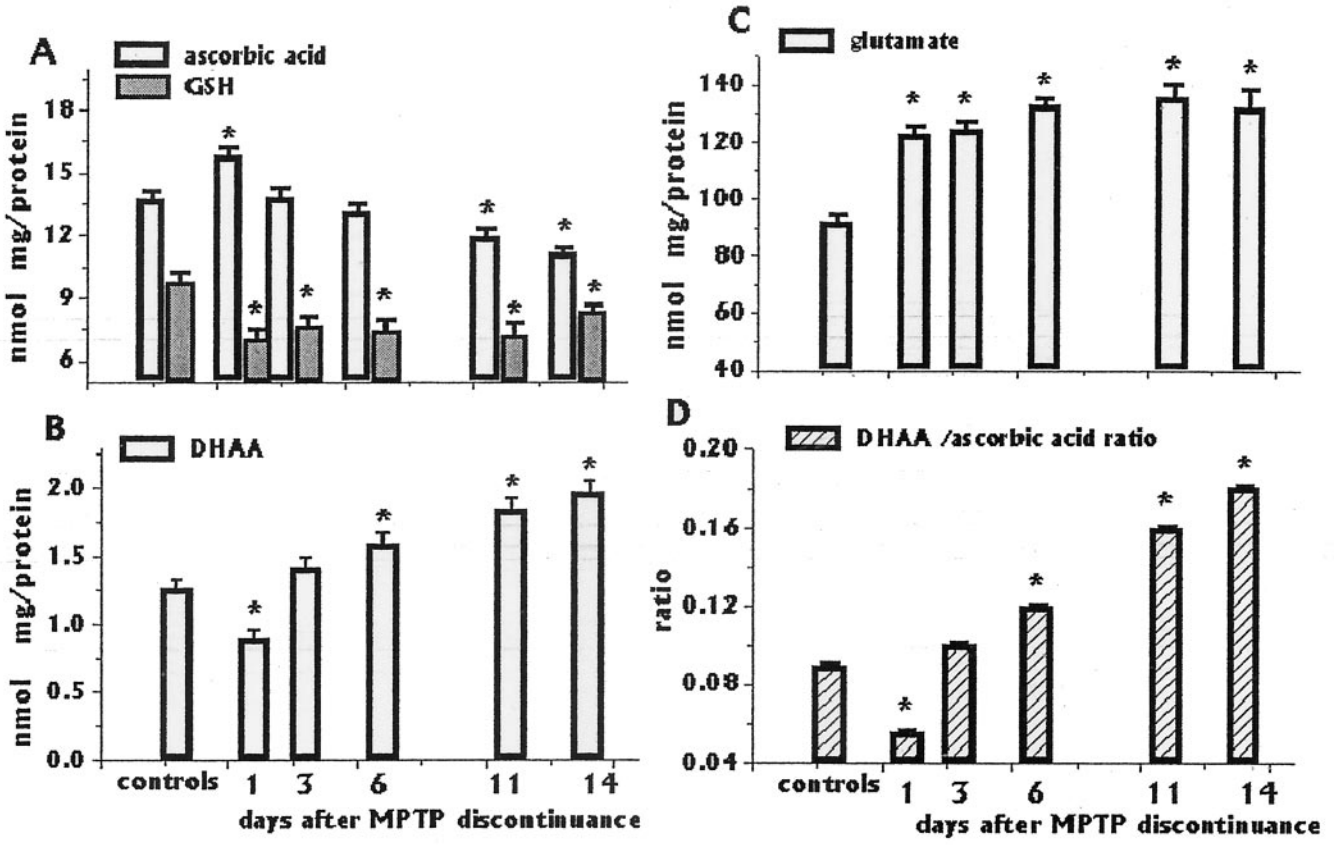

FIG. 3. **Levels of ascorbic acid and GSH (*panel A*), DHAA (*panel B*), glutamate (*panel C*), and the DHAA/ascorbic acid ratio (*panel D*) in the striatum of mice on different days after MPTP discontinuance.** Groups of 8 mice per time period received intraperitoneal injections of MPTP-HCl, 30 mg/kg/day, at 24-h intervals on 5 consecutive days. Mice were killed on the indicated days after MPTP discontinuance. Striatal neurochemical determinations were performed by HPLC on striata of the *left side*. The control group ($n = 11$) was given saline. Values are given as mean ± S.E. *, $p < 0.05$ *versus* controls (ANOVA followed by Student-Neuman-Keul's post-hoc comparison).

pared with controls) (Fig. 1, *panels A* and *B*). DOPAC + HVA levels and the (DOPAC + HVA)/dopamine ratio (Fig. 1, *panels A*, C) were increased further. Ascorbic acid levels had decreased by about 19% (Fig. 3, *panel A*), whereas DHAA levels increased by about 55% (Fig. 3, *panel B*); consequently, the DHAA/AA ratio increased by about 100% (Fig. 3, *panel D*). Changes in GSH (Fig. 3, *panel A*) and glutamate (Fig. 3, *panel C*) levels did not differ from those of day 11. The increase in inosine, hypoxanthine, xanthine, and uric acid levels tended to subside (Fig. 4, *panels A*, *C*, and *D*). In addition, the inosine/hypoxanthine ratio was in the control range (Fig. 4, *panel B*).

At this time point (day 14), both striatal and nigral sections showed a clear regression of gliosis (Fig. 5, *panels g* and *h*). In addition, both striatal and nigral sections showed a noticeable reduction in the number of TUNEL-positive cells, as compared with day 11. Thus, the reduction of the number of TUNEL-positive cells in the striatum was concomitant with the tendency to return to control values of all compounds associated with high-energy phosphate degradation. Hoechst 33342 staining of SNc sections showed few glial cells with condensed chromatin and neurons with presumptive normal morphology (Fig. 7, *panel g*). AO staining of SNc sections showed some glial cells with clumps of hypercondensed chromatin (apopoptic feature), and some neuronal cells with bright orange cytoplasmic fluorescence (presumptive of cellular integrity) (Fig. 7, *panel h*).

DISCUSSION

The results of this study show that a sequential linkage of striatal neurochemical and nigrostriatal cellular events occurs following the discontinuation of a MPTP treatment schedule that is unable to induce necrotic cell death (9). Early (1 day) after MPTP discontinuance, striatal dopaminergic functioning appears to be impaired, as revealed by decreases in striatal dopamine and 3-MT levels and TH activity. However, no clear sign of nigral cell loss, as well as of striatal energy failure, could be detected at this time point. Thus, early MPTP-induced impairment of striatal dopaminergic functioning appears to be unrelated to both nigral neuronal loss and energy failure. The decline of striatal dopamine content in Parkinson's disease has been thought to arise solely from the severe loss of nigrostriatal neurons. However, the striatal dopamine deficit is greater than that presumable on the basis of the loss of nigral neurons (43), suggesting either impaired dopamine synthesis before neuronal degeneration (32), or an increase in striatal dopamine nonenzymatic oxidation and catecholamine conjugates formation (44, 45), or both. Studies in animal models of Parkinson's disease demonstrate that the decrease in the markers of the striatal dopamine metabolism is far greater than the loss of nigral cell bodies (46). TH is a selective target for nitration following exposure to MPTP with a consequent loss of activity (32); in addition, striatal TH is not nitrated in mice overexpressing copper/zinc superoxide dismutase, thus supporting a critical role for superoxide radicals in TH nitration. Dopamine itself, besides TH, is a direct target of MPTP toxicity, because it has been shown that MPP^+ triggers intracellular dopamine nonenzymatic oxidation (7).

Three days after MPTP discontinuance, clear signs of nigral neuronal loss could be detected. At this time point, however, both striatal dopamine levels and TH activity had significantly recovered up to 80% of control values. It has been shown that following MPTP systemic administration, MPTP and MPP^+

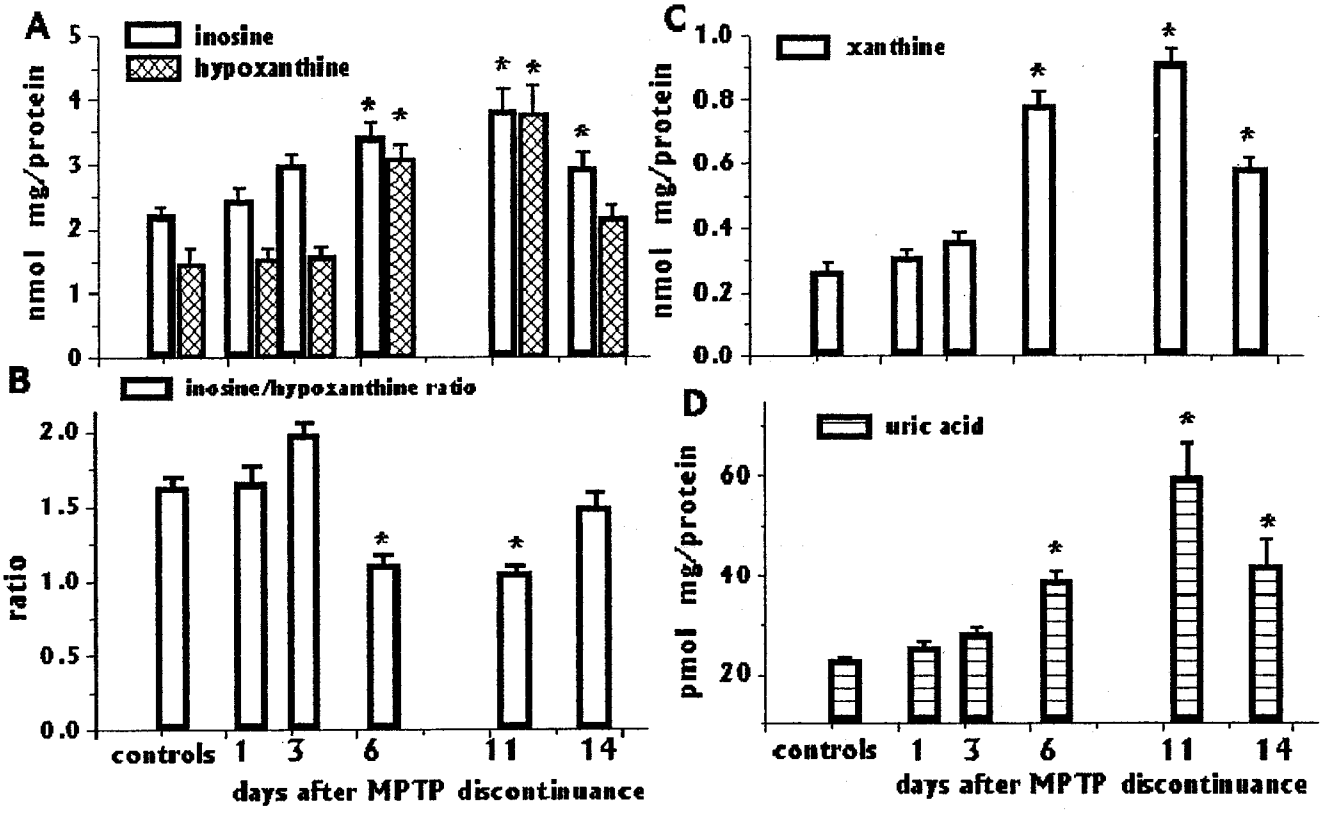

FIG. 4. **Levels of inosine and hypoxanthine (*panel A*), xanthine (*panel C*), uric acid (*panel D*), and the inosine/hypoxanthine ratio (*panel B*) in the striatum of mice at different days after MPTP discontinuance.** Groups of 8 mice per time period received intraperitoneal injections of MPTP-HCl, 30 mg/kg/day, at 24-h intervals on 5 consecutive days. Mice were killed on the indicated days after MPTP discontinuance. Striatal neurochemical determinations were performed by HPLC on striata of the *left side*. The control group ($n = 11$) was given saline. Values are given as mean ± S.E. *, $p < 0.05$ *versus* controls (ANOVA followed by Student-Neuman-Keul's post-hoc comparison).

accumulate neither in the striatum nor in the brainstem, because both are cleared off within 8–24 h (24). Therefore, the transient inhibition of striatal TH activity and the consequent decrease in dopamine levels appear to be linked to the presence of MPP^+ within dopaminergic terminals. These findings further demonstrate that different mechanisms underlie nigral and striatal MPTP toxicity, *i.e.* an early transient impairment of dopaminergic functioning at striatal sites in contrast with delayed nuclear damage at nigral sites. From 6 to 14 days after MPTP discontinuance, both dopamine levels and TH activity failed to recover further; moreover, additional signs of nigral neuronal loss were detected together with massive apoptotic death of nigrostriatal glial cells and striatal neurochemical changes denoting energy failure and increases in ROS formation. It is most likely that these neurochemical changes occur also at the nigral sites (47). The increase in striatal dopamine turnover, as revealed by the increase in the (DOPAC + HVA)/dopamine ratio, suggests that dopamine synthesis in surviving neurons was no longer affected. In reality, it has been shown that MPTP-induced partial loss of striatal dopaminergic TH-immunoreactive fibers results in compensatory sprouting from intact fibers and compensatory changes in the synthesis and metabolism of dopamine (48). Taken together, these findings allow us to speculate that, at these time points, the decline of striatal dopamine content and TH activity might arise solely from the loss of dopaminergic nigral neurons.

The question arises about the mechanism by which MPTP induces loss of nigral neurons at different days after its discontinuance. In fact, TUNEL selectivity in detecting apoptosis in the MPTP *in vivo* model of PD is still a controversial issue (9). In the present study, TUNEL-positive and AO- and Hoechst 33342-stained cells were judged to be apoptotic because of the supportive physical evidence of nuclear condensation obtained with TEM (10).

The late MPTP-induced nigral neuron loss might have been conditioned by the massive glial apoptotic death and increases in reactive radicals formation. A pivotal role of glial pathology in PD disease has recently been outlined (22). There is evidence suggesting that oxidative stress might originate in glial cells rather than in neurons (23) and alterations in glial functioning may be an important contributor to the pathologic process that occurs in PD (22, 49). Glia play a key role in the antioxidant defense of the brain (18) and maintains dopaminergic neuron functioning by supplying trophic factors (19). Today, MPTP-induced activation of resting microglia, and the consequent activation of inducible nitric-oxide (NO) synthase, is believed to be the main culprit of MPTP-induced dopaminergic neuron death (50). Blockade of MPTP-induced microglial activation by means of the tetracycline derivative minocycline mitigates the demise of dopaminergic neurons (50). In PD, activated microglia are found in proximity to damaged nigral cells, suggesting their role in triggering or amplifying neuronal injury as well as in removing the debris of injured cells (51). Lipopolysaccharide-induced activation of the rat nigral microglia is also known to induce the death of dopaminergic neurons (52); in this model, the opioid receptor antagonist naloxone protects nigral neurons without inhibiting microglial activation (52). Lipopolysaccharide-induced activation of microglia results in the release of proinflammatory and neurotoxic factors, such as tumor necrosis factor-α, interleukin-1β, NO, and O_2^- (with a possible downstream formation of peroxynitrite), and hydrogen peroxide. However, only NO and hydrogen peroxide seem to mediate the

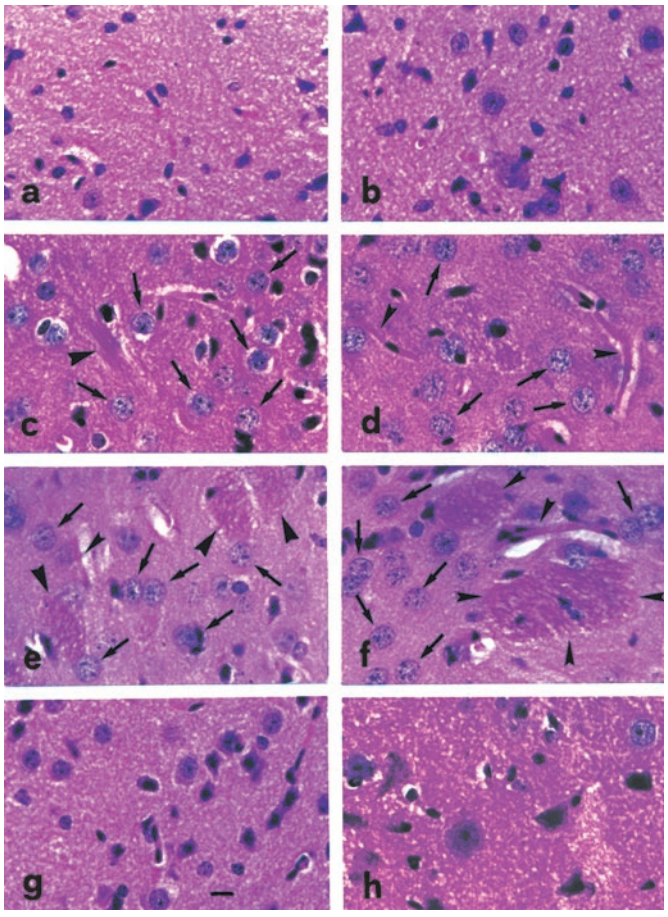

FIG. 5. **Hematoxylin/eosin staining of paraffin sections from striatum (micrographs on *left side*, *panels a*, *c*, *e*, and *g*) and SNc (micrographs on right side, *panels b*, *d*, *f*, and *h*) of mice at different days after MPTP discontinuance.** *Panels a* and *b*, controls. *Panels c* and *d*, 1 day after MPTP discontinuance; a moderate reactive gliosis is revealed by the presence of some enlarged and vesicular nuclei with prominent nucleoli (*arrows*), as well as of eosinophilic Rosenthal fibers (*arrowheads*). *Panels e* and *f*, 6 days after MPTP discontinuance: intense gliosis, as revealed by extensive areas of eosinophilic structures (Rosenthal fibers), indicative of astrocytes arranged in fascicles (*arrowheads*). *Panels g* and *h*, 14 days after MPTP discontinuance: regression of gliosis. *Scale bar*: 20 μm.

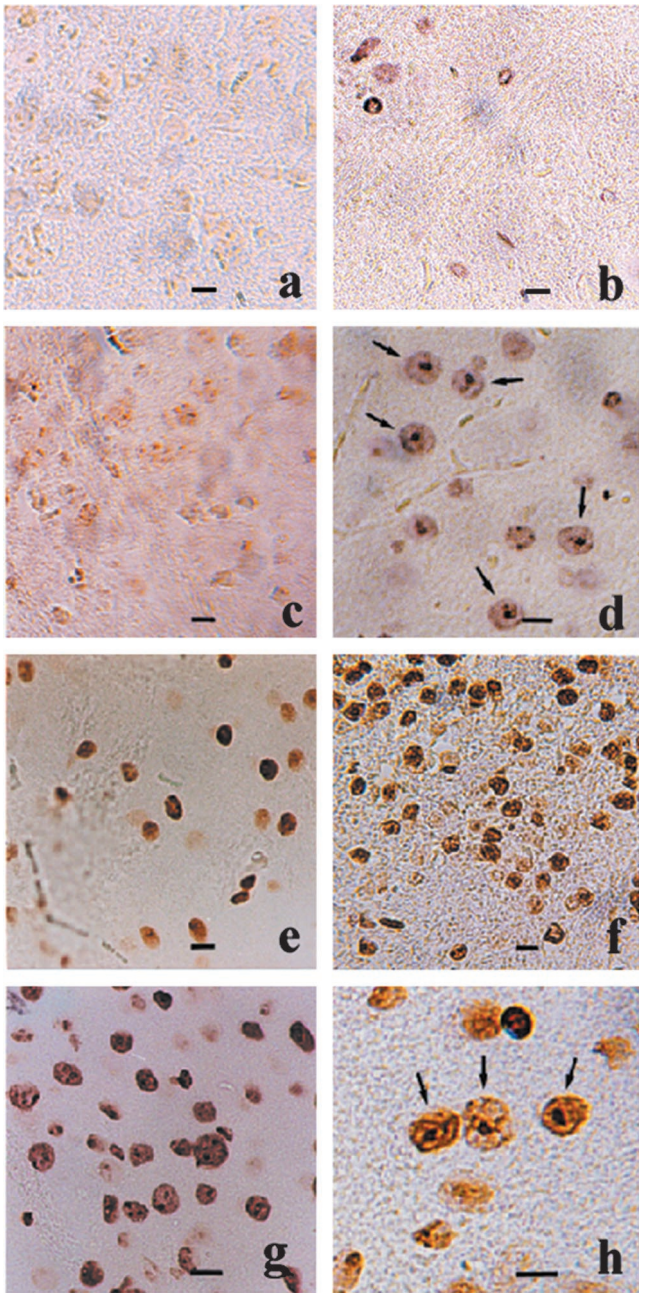

FIG. 6. **TUNEL staining of paraffin sections from striatum (micrographs on *left side*, *panels a*, *c*, *e*, and *g*) and SNc (micrographs on *right side*, *panels b*, *d*, *f*, and *h*) of mice at different days after MPTP discontinuance.** One day after MPTP discontinuance: *panel a*, a section of striatum showing TUNEL negativity; *panel b*, a section of SNc showing some TUNEL-positive cells. Three days after MPTP discontinuance: *panel c*, a section of striatum showing TUNEL negativity; *panel d*, a section of SNc showing some TUNEL-positive cells with nuclei (*arrows*) with neuronal morphology. Six days after MPTP discontinuance: *panel e*, a section of striatum showing several TUNEL-positive cells; *panel f*, a section of SNc showing a great number of TUNEL-positive cells. The increase in TUNEL-positive cells indicates a glial involvement in the apoptotic process. Eleven days after MPTP discontinuance: *panel g*, a section of striatum, showing a number of TUNEL-positive cells greater than on day 6; *panel h*, a section of SNc showing, at higher magnification, some TUNEL-positive cells with nuclei (*arrows*) with neuronal morphology. *Scale bar*: 20 μm.

microglia-induced dopaminergic cell injury (53). Interestingly, lipopolysaccharide-induced activation of astrocytic cultures, coupled with GSH depletion (by means of buthionine-SR-sulfoximine) and complex I inhibition (by means of MPP^+), resulted in extracellular accumulation of NO, hydrogen peroxide, and glutamate (54). In the present study, GFAP immunocytochemistry showed that MPTP-induced reactive gliosis had an astrocytic component, as expected, because astrocytes represent the majority of all glial cells. The activation/apoptotic death of astrocytes, and the presence of nigral neurons with apoptotic features (as revealed by TUNEL positivity, AO and Hoechst 33342 staining, and TEM images of chromatin condensation), occurred in concomitance with decreases in GSH levels, increases in glutamate levels, and increases in compounds associated with high-energy phosphate degradation. Therefore, it is most likely that MPTP-induced activation/apoptotic death of astrocytes may contribute to microglial activation-mediated dopaminergic neuron death, because activated microglia and astrocytes share common cytotoxic mediators (mainly NO and hydrogen peroxide, which are notoriously noted as second messengers in the oxidative stress-induced apoptotic cell death).

Hydrogen peroxide (H_2O_2) is not a free radical, but in the presence of iron it is converted via Fenton reactions to highly reactive hydroxyl radicals, according to the following reactions.

$$H_2O_2 + Fe^{2+} \rightarrow OH\cdot + OH^- + Fe^{3+} \quad (55, 56)$$

REACTION 1

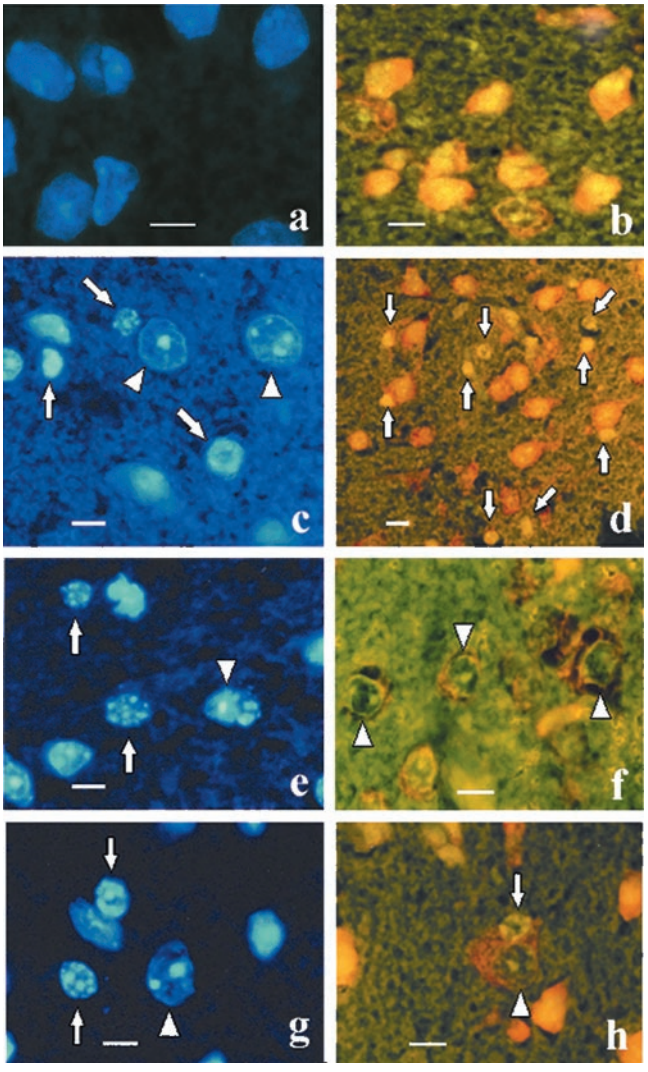

FIG. 7. **Fluorescence microscopy micrographs of mouse SNc at different days after MPTP discontinuance.** Micrographs on the *left side*, *panels a*, *c*, *e*, and *g*, fluorochromization with Hoechts 33342; micrographs on the *right side*, *panels b*, *d*, *f*, and *h*, fluorochromization with AO. *Panels a* and *b*, controls: the bright orange cytoplasmic fluorescence is indicative of cellular integrity (*panel b*). Three days after MPTP discontinuance: *panel c*, the *arrows* indicate chromatin condensation in apoptotic nuclei of glial cells, whereas the *arrowheads* indicate nuclei of apparently normal neurons; *panel d*, the *arrows* indicate pyknotic nuclei of several glial cells (apototic features); the orange cytoplasmic fluorescence is still presumptive of neuronal cells with cellular integrity. Six days after MPTP discontinuance: *panel e*, the *arrows* indicate apoptotic nuclei (apparent clumps of hypercondensed chromatin) of glial cells, whereas the *arrowhead* indicates an apoptotic neuron in which nucleolus-associated chromatin is still evident; *panel f*, the *arrowheads* indicate neurons with condensed chromatin margination at the nuclear periphery associated with pericellular space formation created by cell shrinkage (apoptotic features); in addition, the lack of orange cytoplasmic fluorescence is presumptive of a cellular impairment. Fourteen days after MPTP discontinuance: *panel g*, the *arrows* indicate apoptotic glial cells, whereas the *arrowhead* indicates a normal neuron; *panel h*, the *arrow* indicates an apoptotic glial cell, whereas the *arrowhead* indicates a normal neuron; in addition, the bright orange cytoplasmic fluorescence is presumptive of neuronal integrity.

$$Fe^{3+} + AA \rightarrow Fe^{2+} + DHAA \quad (57)$$

REACTION 2

The above reactions outline the potential role for iron in the pathophysiological cascade of the MPTP-induced neuronal death (56). In reality, misregulation of the iron metabolism and iron-induced oxidative stress are widely believed to be an important pathogenetic mechanism of neuronal death in PD (for review, see Ref. 55).

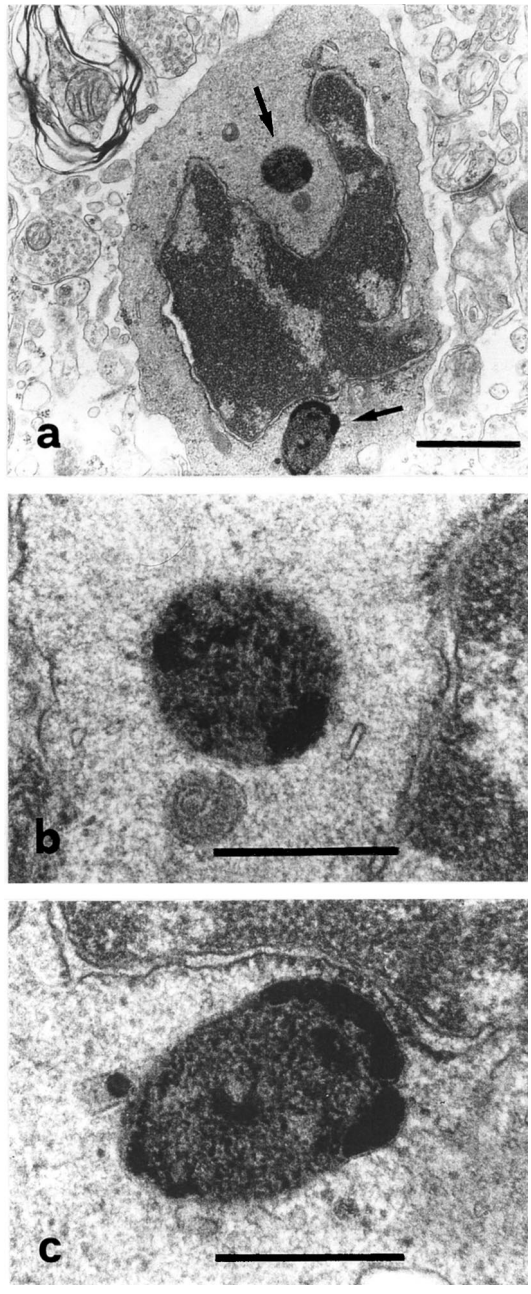

FIG. 8. **TEM micrographs of mouse SNc 6 days after MPTP discontinuance.** A neuron with apoptotic features revealed by chromatin condensation is shown in *a*. The *arrows* indicate membrane-bound structures containing melanin, as shown at higher magnification in *panels b* and *c*. *Scale bar*: 1 μm (*a*) and 0.4 μm (*b* and *c*).

In addition to glial activation-induced generation of NO and ROS, MPTP-induced increases in both dopamine and hypoxanthine/xanthine enzymatic oxidative metabolisms represent a further mechanism of ROS generation. MPTP-induced increases in dopamine and hypoxanthine/xanthine metabolism paralleled the increase in ascorbic acid oxidative status. Enzymatic oxidation of dopamine notoriously generates H_2O_2 (38–40), whereas the enzymatic oxidation of hypoxanthine and xanthine generates O_2^- (41). So far, GSH has been considered the main scavenger of H_2O_2 generated by enzymatic dopamine oxidation (38–40). According to the "radical sink hypothesis," GSH and superoxide dismutase act in a concerted effort to eliminate biologically generated radicals (58). However, the

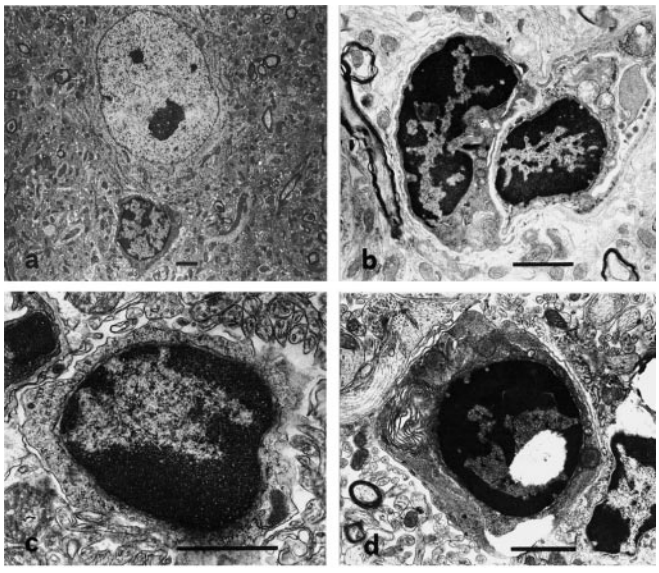

FIG. 9. **TEM micrographs of mouse SNc.** In *panel a* (control), a typical large sized neuron nucleus with dispersed chromatin is visible on the *top*, whereas at the *bottom* a smaller heterochromatic nucleus of a glial cell is visible; glial cells with apoptotic features, as shown by chromatin condensation, are visible in *panels b–d*, 6 days after MPTP discontinuance. *Scale bar*: 1 μm.

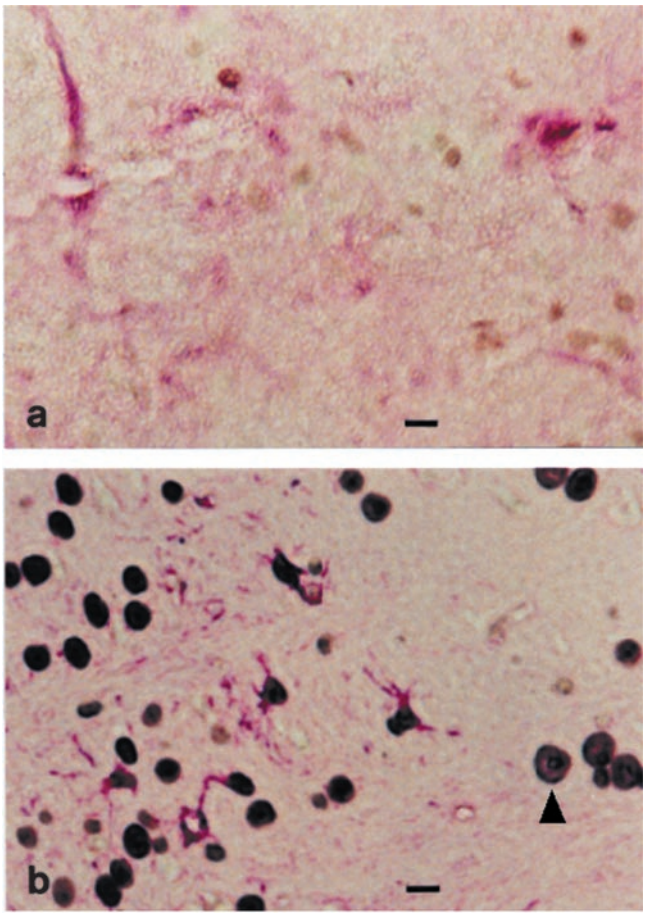

FIG. 10. **GFAP/TUNEL double staining of mouse SNc 6 days after MPTP discontinuance.** Sections were stained with a monoclonal antibody against the GFAP (*red color*) to characterize astrocytes, and stained with TUNEL to characterize the apoptotic nucleus (*brown color*). *Panel a*, a control section showing GFAP positivity but lack of apoptotic nuclei; *panel b*, GFAP-positive cells showing apoptotic nuclei. The *arrowhead* indicates a TUNEL-positive/GFAP-negative cell, which is a neuron, because the nucleus is relatively larger than that of labeled glial cells, and it clearly shows condensed chromatin associated with the nucleolus. *Scale bar*: 20 μm.

physiological relevance of GSH as an antioxidant has been questioned**,** because the ultimate formation of GSSG is preceded by the generation of highly reactive radicals, such as the glutathione thiol radical ($GS^{\bullet}$) and the disulfide radical anion (59). Ascorbic acid can also interact nonenzymatically with H_2O_2 and organic peroxides, but the interaction could also be enzyme-catalyzed (60). In addition, the ascorbate radical is quite unreactive and, unlike $GS^{\bullet}$, is not known to cause any biological damage (61). Ascorbic acid and GSH compartmentalization studies in the brain (62) show an ascorbic acid-to-GSH ratio of 4:1 in neurons (10 *versus* 2.5 mM, respectively), with an opposite ratio of 1:4 in glia (1 *versus* 4 mM, respectively). Sturgeon *et al.* (59) demonstrated that in the presence of physiological concentrations of ascorbic acid and GSH, ascorbic acid, but not GSH, was involved in the detoxification pathway of oxidizing free radicals formed by peroxidase; therefore, ascorbic acid was considered the ultimate radical sink. In the present study, whereas the time course of changes in the ascorbic acid oxidative status paralleled the time course of those of both dopamine and hypoxanthine/xanthine oxidative metabolisms, changes in GSH levels resulted unrelated. In fact, 1 day after MPTP discontinuance, GSH levels had significantly decreased; in contrast, the hypoxanthine/xanthine oxidative metabolism was unchanged, whereas that of dopamine had greatly decreased; in addition, the ascorbic acid oxidative status was significantly decreased. From 3 to 14 days after MPTP discontinuance, the increase in dopamine and hypoxanthine/xanthine oxidative metabolisms strictly paralleled the increase in ascorbic acid oxidative status; in contrast, the decrease in GSH levels was in the range of those observed 1 day after MPTP discontinuance. In a previous study (63), we demonstrated that morphine-induced increases in striatal dopamine and hypoxanthine/xanthine oxidative metabolisms were positively correlated with increases in the ascorbic acid oxidative status. Taken together, these findings strongly support the hypothesis that ascorbic acid may be the ultimate neuronal sink for radicals generated from dopamine and hypoxanthine/xanthine oxidative metabolisms.

The link between dopamine and xanthine metabolisms is as follows (39, 63).

$$\begin{array}{ccccc} O_2 + \text{xanthine (XO)} & \rightarrow & O_2^{\bullet-} & \rightarrow + \text{DA (MAO)} & \rightarrow H_2O_2 \\ & \searrow & & \searrow & \\ & \text{Uric acid} & & \text{DOPAC} & \end{array}$$

REACTION 3

The above link is supported by the finding that allopurinol, a well known inhibitor of xanthine oxidase, inhibits *in vivo* both striatal xanthine and dopamine enzymatic oxidative metabolisms (64–66).

Reports during the past two decades emphasize a key role for GSH in the pathogenesis of Parkinson's disease (23). In PD, postmortem findings show an early decrease (by about 40%) in the nigral levels of GSH (67). However, because dopaminergic neurons make up only 1–2% of the total nigral cell population, and even less in PD, the extent of GSH decreases is too great to take place solely in dopaminergic neurons. This suggests that GSH depletion may occur primarily, if not exclusively, in glial cells (astrocytes and microglia) (54). Much less attention has been paid to ascorbic acid in PD. Postmortem findings showed a significant mean decrease of about 26% of ascorbic acid levels in caudate + globus pallidus + substantia nigra (68). As recalled above, ascorbic acid and GSH compartmentalization studies in the brain give an ascorbic acid-to-GSH ratio of 4:1 in neurons, with an opposite ratio of 1:4 in glia (62). Therefore, if

GSH depletion is thought to occur in PD mainly in glia, that of ascorbic acid may most likely occur in neurons. In the present study, low striatal GSH levels were detected at all time points after MPTP discontinuance. The role of these GSH changes in the pathophysiological cascade of the MPTP-induced neuronal death has yet to be elucidated. GSH depletion by means of buthionine sulfoximine reportedly potentiates MPTP/MPP^+ toxicity to nigral neurons (69, 70); in addition, MPTP is known to induce an early increase *in vivo* in the release of glial GSH, which undergoes hydrolysis in the extracellular compartment (56). This mechanism might account in part for the early MPTP-induced decrease in GSH levels. GSH early depletion, however, may also be related to MPTP bioactivation in astrocytes, a process that generates O_2^- (3). It is quite likely that, in such a case, astrocytic SOD (71) and GSH did act in a concerted effort (58) to eliminate nonphysiologically generated radicals; in addition, it is most likely that astrocytic ascorbic acid did not participate, because 1 day after MPTP discontinuance the ascorbic acid oxidative status had even decreased. However, because MPTP and MPP^+ accumulate neither in the striatum nor in the brainstem, both being cleared off within 8–24 h (24), the mechanism of the late decrease in GSH levels seems to be unrelated to the aforesaid MPTP effects. According to Martenson and Meister (72), one of the important physiological roles of GSH in the central nervous system is to maintain ascorbic acid in its reduced state, because ascorbic acid may have reductive functions that are not efficiently performed by GSH. GSH-dependent reduction of DHAA to ascorbic acid is catalyzed by mammalian glutaredoxin and protein-disulfide isomerase (73). In addition, DHAA may be directly reduced to ascorbic acid by GSH (74). Therefore, GSH-dependent reduction of DHAA to ascorbic acid may be one of the mechanisms underlying late GSH depletion. The above hypothesis is supported by the finding that GSH depletion in newborn rats results in decreases in brain ascorbic acid levels and great increases in DHAA levels (72).

The findings of a MPTP-induced decrease in GSH levels, coupled with increases in DHAA and glutamate levels, also suggest a possible MPTP disrupting effect on the concerted roles of GSH and glutamate in maintaining neuronal ascorbic acid levels. The mammalian brain does not synthesize ascorbic acid, which is supplied from the periphery. Ascorbic acid exists primarily in its reduced form, because DHAA can be readily reduced by enzymatic mechanisms involving semi-DHAA- and DHAA reductase (75), GSH-dependent glutaredoxin, and protein-disulfide isomerase (73). A homeostatic mechanism, demonstrated *in vivo*, keeps striatal extracellular ascorbic acid concentrations (0.2–0.4 mM) constant (76). Extracellular ascorbic acid is actively transported into neurons by means of Na^+-dependent transporters (77), to maintain the estimated concentration of 10 mM. Glia do not have detectable levels of SVTC2, therefore the source of glial ascorbic acid is still uncertain. Glial ascorbic acid is released into the extracellular compartment by means of the glutamate-ascorbate hetero-exchange mechanism, demonstrated *in vivo* by Miele *et al.* (78). Accordingly, glial glutamate uptake results in glial ascorbic acid release into the extracellular compartment. In turn, glutamate taken up by glia may act as a substrate for the synthesis of GSH, which, in turn, ensures glial DHAA reduction back to ascorbic acid by GSH-dependent glutaredoxin and protein-disulfide isomerase (19, 73). Extra-glial DHAA (either released from neurons, or arising from extracellular ascorbic acid oxidation, or both) may be taken up by glia by means of glucose transporters, which are efficient transporters of DHAA (79). MPTP-induced increases in DHAA and glutamate, coupled with decreases in GSH levels, might indicate an impairment of the above recycling mechanism, which is considered an important brain neuroprotective mechanism (80). In the present study, the late decrease in ascorbic acid levels (−13% at day 11, and −19% at day 14), which presumably occurs in neurons, may denote an impairment of those mechanisms ensuring the estimated 10 mM neuronal ascorbic acid concentration.

A glutamatergic mechanism is claimed to be involved in MPTP-induced neurotoxicity (81). NO- and ROS-mediated oxidative stress has long been implicated in the pathogenesis of both acute and chronic *N*-methyl-D-aspartic acid-mediated neurotoxic effects of glutamate (70). In the present study, high tissue levels of glutamate were detected at all time points after MPTP discontinuance. We have no direct evidence of activation of *N*-methyl-D-aspartic acid receptors as a consequence of high tissue levels of glutamate, although it is most likely to occur (70), possibly potentiated by the increased ascorbic acid oxidative status (82); our data allow us to speculate only about the source of glutamate: an early MPTP-induced increase in the release/hydrolysis of glial GSH (56) and a late oxidative-stress mediated inhibition of glial uptake (81).

In conclusion, the results of the present study suggest a sequential linkage of cellular and neurochemical events in MPTP-induced nigral and striatal neurotoxic effects. Early impairment of striatal dopaminergic functioning is transient and unrelated to nigral cell loss. Late nigral cell loss appears to be related to energy failure and seems to recognize interconnected mechanisms in which glia play key mediating roles: NO- and ROS-induced oxidative stress, impairment of cellular antioxidant defense mechanisms, excitoxicity, *i.e.* all those mechanisms currently associated with neuronal death in Parkinson's disease.

REFERENCES

1. Blum, D., Torch, S., Lambeng, N., Nissou, M., Benabid, A. L., Sadoul, R., and Verna, J. M. (2001) *Prog. Neurobiol.* **65,** 135–172
2. Bloem, B. R., Irwin, I., Buruma, O. J. S., Haan, J., Roos, R. A. C., Tetrud, J. W., and Langston, J. W. (1990) *J. Neurol. Sci.* **97,** 273–293
3. Di Monte, D. A., Wu, E. Y., Irwin, I., Delanney, L. E., and Langston, J. W. (1992) *Glia* **5,** 48–55
4. Muralikrishnan, D., and Mohanakumar, K. P. (1998) *FASEB J.* **12,** 905–912
5. Obata, T., and Chiueh, C. C. (1992) *J. Neural Transm.* **89,** 139–145
6. Cassarino, D. S., Fall, C. P., Smith, Y. S., and Bennett, J. P. (1998) *J. Neurochem.* **71,** 295–301
7. Lotharius, J., and O'Malley, K. L. (2000) *J. Biol. Chem.* **275,** 38581–38588
8. Turski, L., Bressler, K., Retting, K. J., Löschman, P. A., and Wachtel, H. (1991) *Nature* **349,** 414–418
9. Tatton, N. A., and Kish, S. J. (1997) *Neuroscience* **77,** 1037–1104
10. Sheehan, J. P., Palmer, P. E., Helm, G. A., and Tuttle, J. B. (1997) *J. Neurosci. Res.* **48,** 226–237
11. Hartley, A., Stone, J. M., Heron, C., Cooper, J. M., and Schapira, A. H. V. (1994) *J. Neurochem.* **63,** 1987–1990
12. Chun, H. S., Gibson, G. E., Degiorgio, L. A., Zhang, H., Kidd, V. E., and Son, J. H. (2001) *J. Neurochem.* **76,** 1010–1021
13. Desole, M. S., Sciola, L., Delogu, M. R., Sircana, S., Migheli, R., and Miele, E. (1997) *Neurochem. Int.* **31,** 169–176
14. Mochizuki, H., Goto, K., Mori, H., and Mizuno, Y. (1996) *J. Neurol. Sci.* **137,** 120–123
15. Anglade, P., Vyas, S., Javoy-Agid, F., Herrero, M. T., Michel, P. P., Marquez, J., Mouatt-Prigent, A., Ruberg, M., Hirsch, E. C., and Agid, Y. (1997) *Histol. Histopathol.* **12,** 25–31
16. Hartmann, A., and Hirsch, E. C. (2001) *Adv. Neurol.* **86,** 143–153
17. Francis, J. W., Von Visger J., Markelonis, G. J., and Oh, T. H. (1995) *Neurotoxicol. Teratol.* **17,** 7–12
18. Wilson, J. X. (1997) *Can. J. Physiol. Pharmacol.* **75,** 1149–1163
19. Lapchak, P. A. (1998) *Mov. Disord.* **13,** 49–54
20. Tomac, A., Lindqvist, E., Lin, L. F., Ogren, S. O., Young, D., Hoffer, B. J., and Olson, L. (1995) *Nature* **373,** 333–335
21. Gash, D. M., Zhang, Z., Ovadia, A., Cass, W. A., Yi, A., Simmerman, L., Russell, D., Martin, D., Lapchak, P. A., Collins, F., Hoffer, B. J., and Gerhardt, G. A (1996) *Nature* **380,** 252–255
22. Banati, R. B., Daniel, S. E., and Blunt, S. B. (1998) *Mov. Disord.* **13,** 221–227
23. Jenner, P., and Olanov, C. W. (1998) *Ann. Neurol.* **44,** Suppl. 3, S72–S84
24. Desole, M. S., Miele, M., Esposito, G., Fresu, L., Migheli, R., Zangani, D., Sircana, S., Grella, G., and Miele, E. (1995) *Pharmacol. Biochem. Behav.* **51,** 581–592
25. Eng, F. L., Lee, Y. L., Kwan, H., Brenner, M., and Messing, A. (1998) *J. Neurosci. Res.* **53,** 353–360
26. Desole, M. S., Serra, P. A., Esposito, G., Delogu, M. R., Migheli, R., Rocchitta, G., and Miele, M. (2000) *Aging Clin. Exp. Res.* **12,** 470–477
27. Anderson, M. E. (1985) *Methods Enzymol.* **113,** 348–355
28. Pothos, E. N., Przedborski, S., Davila, V., Schmitz, Y., and Sulzer, D. (1998)

J. Neurosci. **18,** 5575–5585
29. Lowry, O. H., Rosebrough, N. J., Farr, A. L., and Randall, R. J. (1951) *J. Biol. Chem.* **193,** 265–275
30. Coyle, J. T. (1972) *Biochem. Pharmacol.* **21,** 1935–1944
31. Westerink, B. H. C., and Spaan, S. J. (1982) *J. Neurochem.* **38,** 680–686
32. Ara, J., Przedborski, S., Naini, A. B., Jackson-Lewis, V., Trifiletti, R. R., Horwitz, J., and Ischiropoulos, H. (1998) *Proc. Natl. Acad. Sci. U. S. A.* **95,** 7659–7663
33. Noack, H., Lindenau, J., Rothe, F., Asayama, K., and Wolf, G. (1998) *Glia* **23,** 285–297
34. Hillered, L., Kotwica, Z., and Ungerstedt, U. (1991) *Res. Exp. Med.* **191,** 219–225
35. Zoref-Shani, E., Bromberg, Y., Shirin, C., Sidi, Y., and Sperling, O. (1992) *J. Mol. Cell. Cardiol.* **24,** 183–189
36. Brosh, S., Zoref-Shani, E., Danzinger, E., Bromberg, Y., Sperling, O., and Sidi, Y. (1996) *Int. J. Biochem. Cell Biol.* **28,** 319–328
37. Zoref-Shani, E., Bromberg, Y., Lilling, G., Brosh, S., Sidi, Y., and Sperling, O. (1995) *Int. J. Dev. Neurosci.* **13,** 887–896
38. Maker, H. S., Weiss, C., Silides, D., and Cohen, G. (1981) *J. Neurochem.* **36,** 589–603
39. Chiueh, C. C., Miyake, H., and Wong, P. K. (1993) *Adv. Neurol.* **60,** 251–258
40. Adams, J. D., Jr., Chang, M. L., and Klaidman, L. (2001) *Curr. Med. Chem.* **8,** 809–814
41. Becker, B. F. (1993) *Free Radical Biol. Med.* **14,** 615–631
42. Desole, M. S., Esposito, G., Enrico, P., Miele, M., Fresu, L., De Natale, G., Miele, E., and Grella, G. (1993) *Neurosci. Lett.* **159,** 143–146
43. Pakkemberg, B., Moller, A., Gundersen, J., Mouritzen Dam, A., and Pakkemberg, H. (1991) *J. Neurol. Neurosurg. Psychiatry* **54,** 30–33
44. Rabinovich, A. D., and Hastings, T. (1998) *J. Neurochem.* **71,** 2071–2078
45. Spencer, J. P., Jenner, P., Daniel, S. E., Lees, A. J., Marsden, D. C., and Halliwell, B. (1998) *J. Neurochem.* **71,** 2112–2122
46. German, D. C., Nelson, E. L., Liang, C. L., Speciale, S. G., Sinton, C. M., and Sonsalla, P. K. (1996) *Neurodegeneration* **5,** 299–312
47. Pennathur, S., Jackson-Lewis, V., Przedborski, S., and Heineckel, J. W. (1999) *J. Biol. Chem.* **274,** 34621–34628
48. Song, D. D., and Haber, S. N. (2000) *J. Neurosci.* **13,** 5102–5114
49. McNaught, K. S., Lee, M., Hyun, D. H., and Jenner, P. (2001) *Adv. Neurol.* **86,** 73–82
50. Wu, D. C., Jakson-Lewis, W., Vila, M., Tieu, K., Teisman, P., Vadseth, C., Choi, D.-K., Ischiropoulos, H., and Przedborski, S. (2002) *J. Neurosci.* **22,** 1763–1771
51. McGeer, P. L., Itakagi, S., Boyes, B. E., and McGeer, E. G. (1998) *Neurology* **38,** 1285–1290
52. Lu, X., Bing, G., and Hagg, Y. (2000) *Neuroscience* **97,** 285–291
53. Le, W.-D., Rowe, D., Xie, W., Ortiz, I., He, Y., and Appel, S. H. (2001) *J. Neurosci.* **21,** 8447–8455
54. McNaught, K. S., and Jenner, P. (2000) *Biochem. Pharmacol.* **62,** 979–988
55. Jellinger, K. A. (1999) *Drugs Aging* **14,** 11–140
56. Han, J., Cheng, F-C., Yang, Z., and Dryhurst, G. (1999) *J. Neurochem.* **73,** 1683–1695
57. Berger, T. M., Polidori, M. C., Dabbagh, A., Evans, P. J., Halliwell, B., Morrow, J. D., Jackson Roberts, L., and Frei, B. (1997) *J. Biol. Chem.* **272,** 15656–15660
58. Winterbourn, C. C. (1993) *Free Radical Biol. Med.* **14,** 85–90
59. Sturgeon, B. E., Sipe, H. J., Jr., Barr, P. D., Corbett. J. T., Martinez, J. G., and Mason, R. P. (1998) *J. Biol. Chem.* **273,** 30116–30121
60. Dalton, D. A., Russell, S. A., Hanus, F. J., Pascoe, G. A., and Evans, H. J. (1986) *Proc. Natl. Acad. Sci. U. S. A.* **83,** 3811–3815
61. Biolski, B. H. J. (1982) in *Ascorbic Acid: Chemistry, Metabolism, and Use* (Seib, P. A., and Tolbert, B. M., eds) pp. 81–100, American Chemical Society, Washington, D. C.
62. Rice, M. R. (1999) *Neurotoxicity Res.* **1,** 81–90
63. Desole, M. S., Esposito, G., Fresu, L., Migheli, R., Enrico, P., Mura, M. A., De Natale, G., Miele, E., and Miele, M. (1996) *Brain Res.* **723,** 153–161
64. Miele, M., Esposito, G., Sircana, S., Zangani, D., Migheli, R., Fresu, L., and Desole, M. S. (1995) *Neurosci. Lett.* **183,** 155–159
65. Enrico, P., Esposito, G., Mura, M. A., Migheli, R., Serra, P. A., Desole, M. S., Miele, E., De Natale, G., and Miele, M. (1997) *Pharmacol. Res.* **35,** 577–585
66. Church, W. H., and Rappolt, G. (1999) *Exp. Brain Res.* **127,** 147–150
67. Sian, J., Dexter, D. T., Lees, A. J., Daniel, S., Agid, Y., Javoy-Agid, F., Jenner P., and Marsden, C. D. (1994) *Ann. Neurol.* **36,** 348–355
68. Riederer, P., Sofic, E., Rausch, W.-D., Schmidt, B., Reynolds, G. P., Jellinegr, K., and Youdim, M. B. H. (1989) *J. Neurochem.* **52,** 515–520
69. Wüllner, U., Löschmann, P. A., Schulz, J. B., Schmidt, A., Dringen, R., Eblen, F., Turski, L., and Klockgether, T. (1996) *Neuroreport* **7,** 921–923
70. McNaught, K. P., and Jenner, P. (1999) *J. Neurochem.* **73,** 2469–2476
71. Savolainen, H. (1998) *Res. Commun. Chem. Pathol. Pharmacol.* **21,** 173–176
72. Martenson, J., and Meister, A. (1991) *Proc. Natl. Acad. Sci. U. S. A.* **88,** 4656–4660
73. Wells, W. W., Xu, D. P., Yanf, Y., and Rocque, P. A. (1990) *J. Biol. Chem.* **265,** 15361–15364
74. Guaiaquil, V. H., Farber, C. M., Golde, D. W., and Vera, J. C. (1997) *J. Biol. Chem.* **272,** 9915–9921
75. Diliberto, E. J., Menniti, F. S., Knoth, J., Danield, A., Kizer, J. S., and Viveros, H. O. (1992) *J. Neurochem.* **39,** 363–368
76. Miele, M., and Fillenz, M. (1996) *J. Neurosci. Methods* **70,** 15–19
77. Tsukaguchi, H., Tokui, T., Mackenzie, B., Berger, U. V., Chen, X. Z., Wang, Y., Brubaker, R. F., and Hediger, M. A. (1999) *Nature* **399,** 70–75
78. Miele, M., Boutelle, M., and Fillenz, M. (1994) *Neuroscience* **62,** 87–91
79. Vera, J. C., Coralia, I. R., Velàsquez, F. V., Zhang, R. H., Concha, I. I., and Golde, D. W. (1995) *J. Biol. Chem.* **270,** 23706–23712
80. Rice, M. E. (2000) *Trends Neurosci.* **23,** 209–219
81. Trotti, I. D., Danbolt, N. C., and Volterra, A. (1998) *Trends Pharmacol. Sci.* **19,** 328–334
82. Kiyatkin, E. A., and Rebec, G. V. (1998) *Brain Res.* **812,** 14–22

The Neurotoxin 1-Methyl-4-phenyl-1,2,3,6-tetrahydropyridine Induces Apoptosis in Mouse Nigrostriatal Glia: RELEVANCE TO NIGRAL NEURONAL DEATH AND STRIATAL NEUROCHEMICAL CHANGES

Pier Andrea Serra, Luigi Sciola, Maria Rosaria Delogu, Alessandra Spano, Gianni Monaco, Egidio Miele, Gaia Rocchitta, Maddalena Miele, Rossana Migheli and Maria Speranza Desole

J. Biol. Chem. 2002, 277:34451-34461.
doi: 10.1074/jbc.M202099200 originally published online June 25, 2002
